Dielectric behavior and physico-chemical properties of 60 kV HV crosslinked polyethylene under long-term electrical aging

Abdelhay Smaida[1], Yacine Mecheri[1], Larbi Boukezzi[2,*], Slimane Bouazabia[1]

[1]LSEI Laboratory, USTHB, Algiers, Algeria
[2]Materials Science and Informatics Laboratory, MSIL, University of Djelfa, Djelfa 17000, Algeria
*Corresponding Author - E-mail: larbiboukezzi@gmail.com

ABSTRACT

This study focuses on the study of long-term electrical aging effects on dielectric behavior of cross-linked polyethylene (XLPE) used as insulation in high voltage cables. For this reason, we have performed long-term electrical aging tests on full size of HV 36/60 kV XLPE cable samples at three voltage levels ($U_0 = 36$ kV, $2U_0 = 72$ kV and $3U_0 = 108$ kV) during 680 hours. The studied properties are partial discharge threshold, dielectric loss factor, relative permittivity and transverse resistivity. Besides, physico-chemical changes were assessed using Fourier Transform Infrared Spectroscopy (FTIR) and X-ray diffraction (XRD). In addition, complementary diagnostic measurements, including mechanical characterization and visual observation analysis are carried out in the end of this paper. The obtained results illustrate that examined properties are widely affected by long-term electrical aging. The increase in partial discharges and dissipation factor depending to the voltage level and the aging time and the decrease in partial discharge threshold voltage and transverse resistivity are the mostly marked degradation precursors. These degradation precursors are supported by the increase of carbonyl groups and reduction in the crystallinity degree of the polymer under long-term electrical aging. These parameters are useful parameters for evaluating the quality of underground XLPE cable insulator.

INTRODUCTION

Cross-linked polyethylene (XLPE) has become the preferred material for main insulation in high voltage cables. This material has replaced other types of polyethylene thanks to its excellent electrical, and its mechanical and thermal properties, and maintaining the basic insulating performances of other kinds of polyethylene. This excellent insulation material, commonly used in high voltage cables, is characterized by a very high dielectric strength and low dielectric losses [1]. However, it is well known that this material may undergo dramatic alteration on their properties when exposed to stress under service conditions. These constraints limit the performance of this insulation, alter their properties (dielectric, mechanical, chemical…etc), cause irreversible damage and lead to its aging.

Degradation under service conditions is the major problem of XLPE high voltage cables. During service, XLPE cable is affected by many factors, such as thermal oxidative aging, high electric field, electrode deterioration…etc. This will lead to irreversible aging damage [2,3]. Many scholars have put in evidence that electrical stress is one of the harmful destructive factors that affecting XLPE insulating performances. The degradation phenomenology claimed that when the electric field intensity exceeds the threshold value, the molecular chain breaking is

accelerated, and the structure of cross-linked polyethylene is destroyed. Hence, new free paths are created which is easy to cause electric breakdown [4]. In literature, a lot of work has been carried out in this subject. For example, Stancu et al. [5] have shown that electrical aging associated to the presence of water may lead to growth of water trees. Li et al. [6] have investigated the influence of different aging modes on the space charge dynamics and physicochemical properties of XLPE insulated cables. Li et al. [7] have made research on the degradation in micro-structure and dielectric performance of XLPE cable insulation in service. Wang et al. [8] have concluded that partial discharges are the result of space charge accumulation in polyethylene under high voltage DC field. However, achieved results from these investigations ascertain that only change of dielectric performances can't obviously clarify the microscopic origin of the aging evolution under applied stress. Therefore, combination of many laboratory tests based on microscopic physico-chemical analysis with the observed macroscopic bulky evolution of dielectric performances is mandatory. The relevance of the use of physico-chemical analysis to quantify the degradation degree of XLPE after aging was well highlighted in the literature. The use of Fourier transforms infrared spectroscopy (FTIR) helps in the better understanding of electrical behavior (like space charge initiation and accumulation) of XLPE under long-term electrical aging. It was ascertained in [6] that FTIR measurements are very sensitive to the chemical changes like free radicals creation and oxidized groups. Besides, it was highlighted that the use of differential scanning calorimetry (DSC) can help to reveal details on the crystalline nature and crystallinity degree alteration of XLPE caused by electrical aging. In reference [6], it was found that under service conditions for long time more than 22 years leads to the reduction in the lamellae thickness and crystallinity degree. Supplementary informations are gained from the use of X-ray diffraction on the crystalline phases of XLPE under aging as highlighted in [7].

The aim of this paper is in line with this philosophy. It consists to comprehensively evaluate the effects of long-term electrical aging on XLPE high voltage insulation by providing quantitative relationships between voltage levels, aging time and various characteristics such as electrical, physico-chemical and mechanical characteristics.

EXPERIMENTAL

Materials and sampling

Samples of 10 meters full size length were taken from a final industrial cable product. This cable is intended to be used in 60 kV high voltage network. The main insulation is XLPE crosslinked under hot inert nitrogen. The complete constitution of the cable specimens is shown in Figure 1.
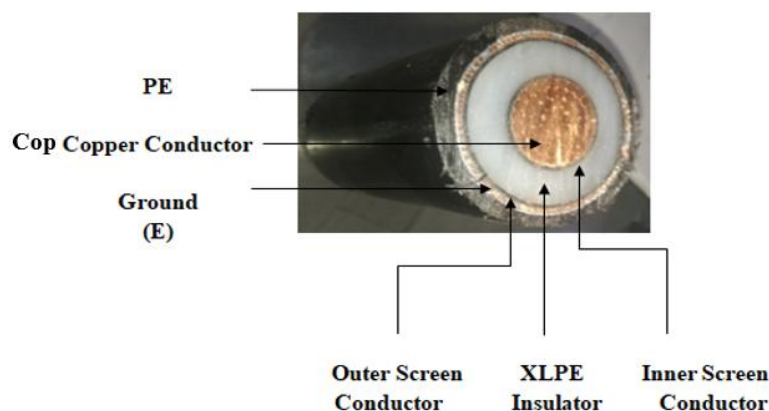

PE

Cop Copper Conductor

Ground (E)

Outer Screen Conductor   XLPE Insulator   Inner Screen Conductor

Figure 1. HV 36/60 kV XLPE insulated cable.

The final cable exhibits the following characteristics listed in Table 1.

Table 1. Cable characteristics.

Cable type	630 mm² Cu 36/60 (66) kV
Core : Inner radius R_1	15.03 mm
XLPE insulation thickness	11 mm
Outer radius R_2	27.35 mm
XLPE permittivity	2.3
Normal allowed temperature	90 °C
Emergency temperatures	150 °C – 250 °C

Electrical aging

Separately, the full size 10 m length of HV 36/60 (66) kV XLPE cable samples above-described were subjected to accelerated endurance electrical aging tests. 50 Hz AC voltage stress were applied on each sample during 680 hours. Three voltage levels were chosen: U_0, $2U_0$ and $3U_0$ corresponding to 36 kV, 72 kV and 108 kV respectively.

The experimental circuit is consisted of an autotransformer, a step-up transformer with 50 Hz power frequency, a protection resistor, a capacitive voltage divider and a coupling capacitor (Figure 2).
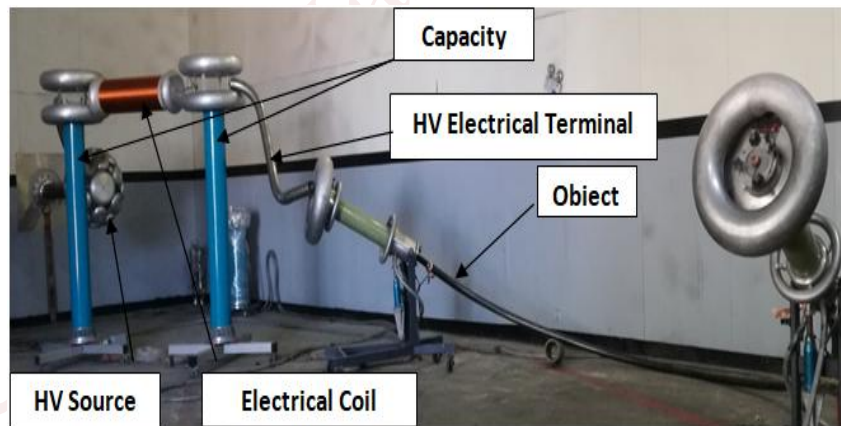

Figure 2. Electrical testing circuit in laboratory.

Dielectric tests

A schematic presentation of the test setup for measuring the threshold voltage of partial discharges, dissipation factor and capacitance is given in Figure 3. The measurement of each parameter is done after 170 hours of aging. The threshold voltage of partial discharges is measured according to IEC60270 Standards [9]. As for the partial discharges, dissipation factor and the capacitance are measured according to IEC60840 Standards [10].The smallest detectable charge in partial discharges measurements was 1 pC. The test voltage was applied

between the copper conductor and the copper screen (shield) of the cable according to IEC 60840 Standards [10]. The test voltages were increased from 0.5Uo to 2.5Uo for partial discharges and from 10 kV to 70 kV for dissipation factor and capacitance.

Schering bridge

The dielectric losses factor ($tan\delta$) was measured as a function of the voltage by using a Schering bridge (AG type TG-3MOD) under the ambient temperature and the frequency of 50 Hz. The test consists to place the conductive core on the HV terminal of the transformer and the metal screen to earth, and then gradually increase the test voltage. A filter containing an inductor and two parallel capacitors were used to reduce background noises and a layer of semi-insulating paint was applied through the surface of the cable ends to reduce the leakage currents.
The relative permittivity is calculated using the following relation:

$$\varepsilon_r = \frac{C_x}{2\pi\varepsilon_0 \dfrac{l}{ln\dfrac{r_2}{r_1}}} \tag{1}$$

Where C_x is the capacitance of the sample between the core and the shield conductor, l is the length of the sample, ε_o is the permittivity of the vacuum ($\varepsilon_o = 8.85\text{x}10^{-12}$ Fm^{-1}) and r_2 and r_1 are the outer and inner radius of sample.
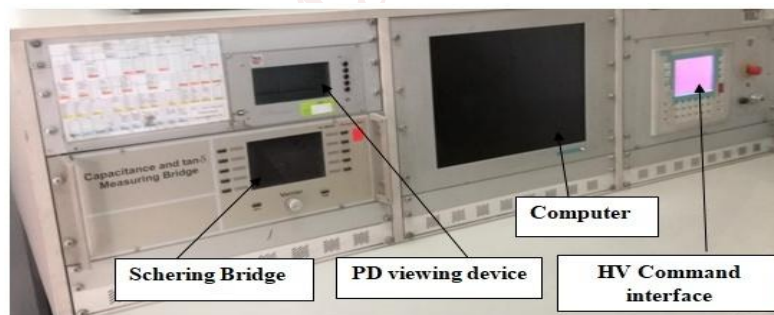

Figure 3. PD and *tanδ* measurement devices.

Transverse resistivity measurement

The transverse resistivity measurement is carried out in electrical test laboratory of Elsswedy Company (Algeria), using a MIT510/2 type Megohmmeter, applying 500 V DC voltage for 10 minutes. The insulation resistance is measured then the transverse resistivity is calculated using the following relation:

$$\rho = \frac{2\pi R l}{ln\dfrac{r_2}{r_1}} \tag{2}$$

Where R is the insulation resistance of the sample between the core and the shield conductor, l is the length of the sample thickness and r_2 and r_1 are the outer and inner radius of sample.

Optical microscopy observation

Optical microscopy images were acquired using a leica DM2500 M associated with CCD camera for digital image acquisition. The images were taken through a 5x objective lens and 10x eye piece.

Fourier transforms infrared spectroscopy (FTIR)

The structural changes of XLPE caused by long-term electrical aging were analyzed with the IRAffinity-1s SHIMADZU spectrometer model driven by IRsolution software and fitted with an Attenuated Total Reflectance (ATR) accessory. The samples have a relatively large thickness, of the order of 1.6 mm; which made it necessary to use the FTIR analysis in Attenuated Total Reflection (ATR) mode. Each sample was performed at 32 scans in range 400-4000 cm^{-1} with a resolution of 4 cm^{-1} to increase the accuracy of the results.

X-ray Scattering

To make clear any changes in the crystalline phase of XLPE caused by long-term electrical aging, an X-ray diffraction has been used. An X'PertPro MPD/Panalytical diffractometer (goniometer radius 240 mm) equipped with a PIXcel 1D detector was used to record the DRX spectra. These were recorded in standard mode (θ-θ) in the angular range from 12 to 65° (2θ) with a step of 0.0263° and an acquisition time of 38 s. A copper anticathode was used as the source of radiation K_α= 0.1540598 nm. The power of the used radiation is 30 kV and 40 mA. The diffractometer was connected to a computer in order to receive and analyze the data. The data obtained was analyzed by the X'Pert Graphics Identifier software.

Mechanical Tests

Elongation at break and tensile strength

The mechanical behavior is characterized by the measurement of the elongation at break and tensile strength using a tensile machine (Zwickroell, Germany) (Figure 4) in accordance with IEC standard [11]. This machine has an adjustable drive to perform the tests at controlled speed. It is equipped with two jaws; one fixe and the other mobile, as well as force sensors to determine the force required to break the specimen. The machine is controlled by software where the parameters can be entered by computer. The speed of the mobile jaw is set at 25 mm/min.

Figure 4. Uniaxial tensile testing machine.

Hot set test

The change in the degree of cross-linking is estimated by a hot elongation test (Hot set test). The test is carried out in an oven maintained at 200 °C. Also, the samples are suspended vertically in the oven and subjected to a load of 20 N/cm² attached with jaws to the lower end of the test pieces. After 15 minutes at 200 °C in the oven the distance between the reference lines is measured and the percentage elongation is calculated in accordance with IEC standard [12].

RESULTS AND DISSCUSSIONS

Results of dielectric properties

Dielectric properties are the most helpful indicators to evaluate degradation under long-term electrical aging. The evolution of these properties according to aging time and applied voltage levels are given in the next sections. The studied dielectric properties are partial discharges threshold voltage, partial discharges amount, dissipation factor, relative permittivity and transverse resistivity.

Threshold voltage of partial discharges

Figure 5 shows the influence of electrical aging on the evolution of the partial discharge threshold voltage U_{pdv}. It can be seen from the curves that PD threshold voltage decreases with aging time. This decrease seemed more marked when the level of the applied voltage is higher. A value greater than 61 kV was observed in the case of the unaged samples, which is the highest value of the threshold voltage for partial discharges. It is due to the larger amounts of peroxide decomposition effect which acts as a voltage stabilizer in this case [13]. A decrease in the threshold voltage of partial discharges reveals on the degradation of the insulating material, which causes, with time, changes in its structure, electrical and physical properties especially under high stresses transient situation due to overvoltage. Under the investigated voltage stresses, the obtained change rates on the PD voltage were 18.5 %, 24.6 %   and 41 % respectively.
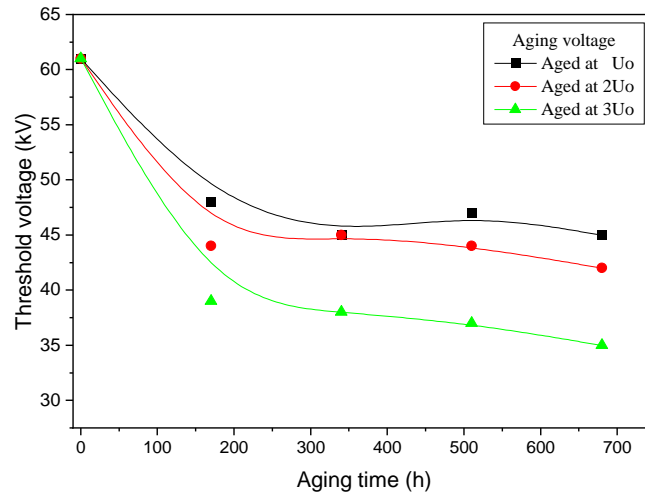
Figure 5. Threshold voltage as a function of aging time.

Partial discharges

Partial discharges were measured according to the aging time and applied test voltage for all voltage aging levels (U_0, $2U_0$ and $3U_0$). The obtained results are depicted in Figures 6(a to d). It is very clear from these figures that before aging, partial discharges present little increases with increasing applied test voltage up to $1.7U_0$ (61.5 kV). After $1.7U_0$, a marked fast increase of partial discharges is observed which reaches 3 pC for an applied voltage of 2.5 U_0 (90 kV). The voltage of $1.7U_0$ can represent the threshold of ionizing process in fresh 60 kV XLPE insulation. Furthermore, the threshold of ionization in the aged samples is reduced to U_0 (36 kV) where partial discharges increase speedily when higher voltage than this threshold value is applied. After 680 h of aging under U_0, $2U_0$ and $3U_0$, partial discharges reach 5.7 pC, 5.9 pC and 6.67 pC respectively. The higher aging voltage leads to greater partial discharges amount. This result is in line with the Jonscher's model based on percolation concept [14]. This concept claimed that over the aging period, the applied electric field leads to the enhancement of defects density like vacuoles, holes and unsaturated groups. Hence, more partial discharges occurred before the final breakdown of the material which may explain the increase trends of partial discharges curves in Figure 6. Besides, the occurrence of partial discharges leads to the temperature rising within vacuoles which causes the oxidation of their walls as claimed by many researchers [15].
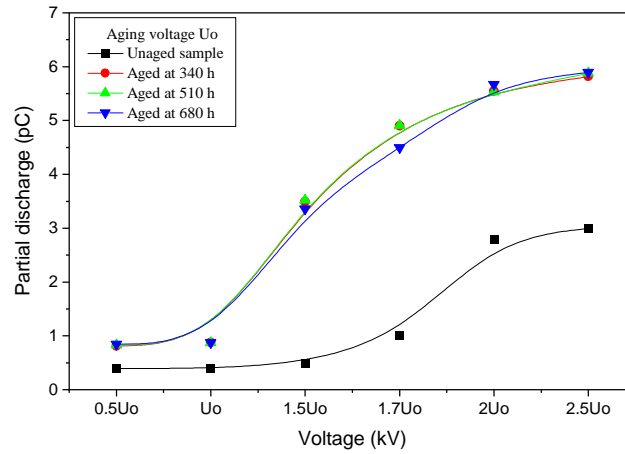
Figure 6a. Partial discharges versus applied voltage before and after aging at U_o.
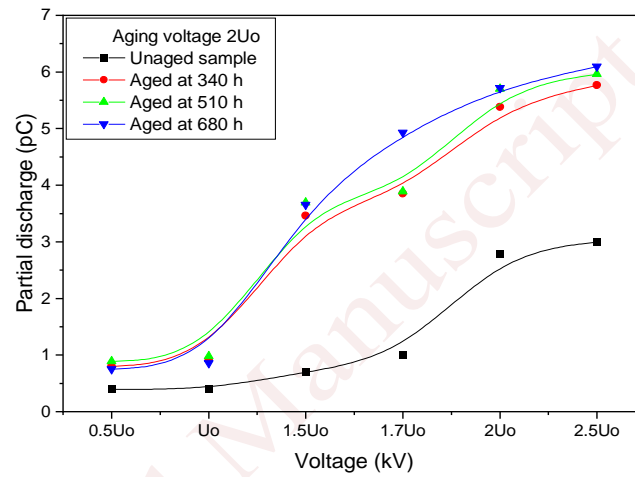

Figure 6b. Partial discharges versus applied voltage before and after aging at $2U_o$.
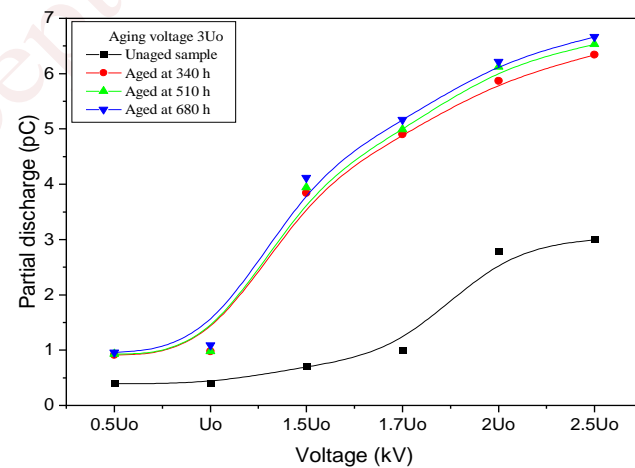

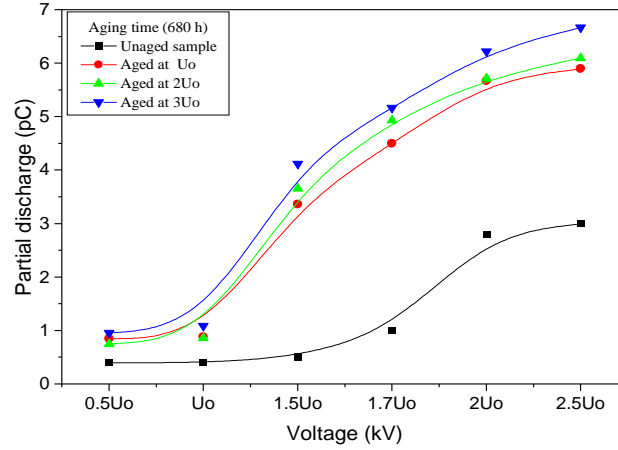**Figure 6c.** Partial discharges versus applied voltage before and after aging at $3U_o$.

Figure 6d. Partial discharges versus applied voltage before and after aging.

Dissipation factor

Dissipation factor (*tanδ*) variations according to the applied voltage and aging time are shown in Figures 7(a to d). The same behavior was observed for all samples where the dissipation factor increases with both aging time and test voltage. If we take for example the applied voltage U_0, *tanδ* of the unaged samples is about 0.005 which is less than the upper limit tolerated by IEC-60840 Standards [10]. One can note also that the values of *tanδ* increase with increasing electrical aging voltage. After 680 h of aging it passes to 0.0193 after aging at U_0 and reaches 0.0515 and 0.0521 after aging at $2U_0$ and $3U_0$ respectively. All of these values are higher than the upper limit tolerated by IEC-60840 Standards [10]. Figure 6 highlights clearly that as aging became more severe (in time and in applied voltage level), more polar products were generated in the XLPE insulation. As the voltage amplitude increased, the polarization process became more complete, resulting in greater losses in the bulk of the material [16,17].

Based on the obtained results, *tanδ* increases considerably from a critical value of voltage level of 30 kV which could be the ionization threshold, beyond which partial discharges appear in the material resulting in significant dielectric losses increasing [18]. In addition, dissipation factor mainly depends on the electrical conductivity and dipole polarization [19]. Therefore, it can be considered the sum of several kinds of losses caused by the presence of impurities, oxidized products and orientation of dipoles associated with morphology [20].
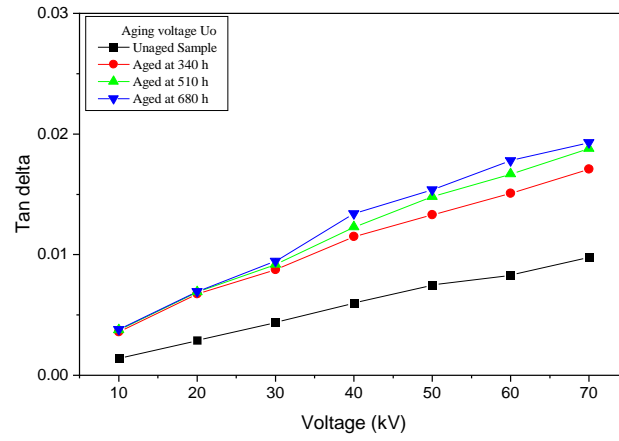
Figure 7a. Dissipation factor versus applied voltage before and after aging at U_0.
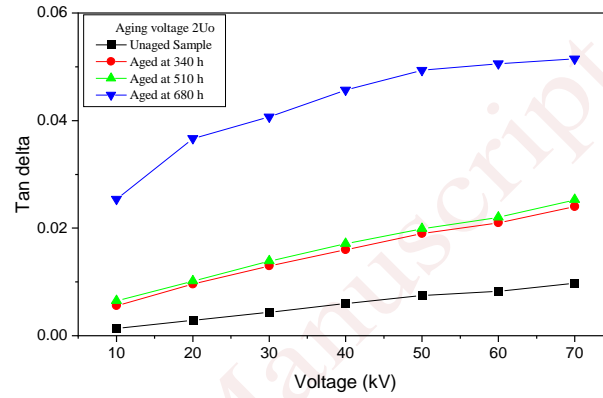

Figure 7b. Dissipation factor versus applied voltage before and after aging at $2U_0$.
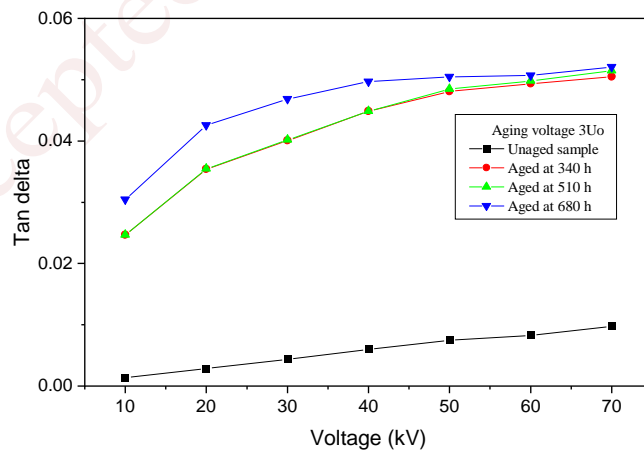

Figure 7c. Dissipation factor versus applied voltage before and after aging at $3U_0$.
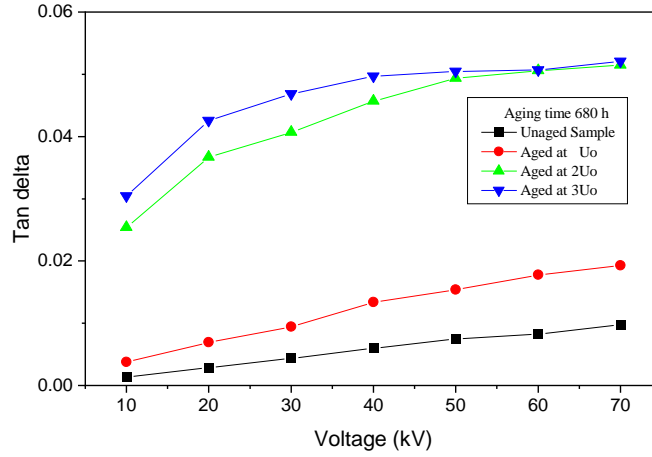
Figure 7d. Dissipation factor versus aging time and applied voltage.

- Degradation degree of XLPE based on tanδ assessment

In electrical insulation industry, *tanδ* is considered as a crucial indicator of degradation. The degradation degree can be evaluated through two parameters: degradation index (DI) and degradation rate (DR). DI evaluates the overall degradation and DR indicates the relative change in the cable performance between two consecutive measurements. Both parameters are given by Equations (3) and (4) respectively [21]:

$$DI_k = \frac{Stang\delta_k}{Stang\delta_0} \tag{3}$$

$$DR_k = \frac{Stang\delta_k}{Stang\delta_{k-1}} \tag{4}$$

With:

Stanδ$_k$ is the surface enclosed by the *tanδ* curve at aging time k.

Stanδ$_0$ is the initial surface at time 0

Stanδ$_{k-1}$ is the surface enclosed by *tanδ* curve at aging time k-1.

We have depicted the DI and DR curves for different aging time and for three aging voltage levels. The depicted characteristics concern two values off applied testing voltage 40 kV (the nearest to U$_0$) and 70 kV (nearest to 2U$_0$). Figures 8 and 9 show the obtained results.

From Figure 8, it is very clear that DI has similar trends for both tested voltages. It increases with the increase of aging time to reach somewhat a steady state in the case of aging at U$_0$ and 3U$_0$ (Figure 8a and 8c),while it follows its continuous increasing trend in the case of aging at 2U$_0$. The important increase of DI is observed after the first 340 h of aging in the case of U$_0$ and 3U$_0$ where it reaches the value of 1.9 and 7.5 respectively for an applied voltage of 40 kV. On the other hand, the important increase is mentioned after 680 h of aging at 2U$_0$. To be in accordance with previous literature [21], the DI value of 1.5 was recognized as a critical threshold for the level of degradation of XLPE insulation, so obtained results highlight that this value is widely overlapped after the first 340 h of aging and sometimes before this time. These results indicate that electrical aging has a significant impact on the alteration of structure and

chemistry of XLPE. Oxidation reactions, creations of defects and holes, and generation of dipoles are the main causes of the important increase of DI values.

Since DI represents the cumulative degradation process, DR represents the happening gradual degradation in the material. The depicted results in Figure 9 are in agreement with the variation of DI. It is clear that the highest values were noticed after 340 h of aging which corresponds to the fast increase of DI values. The critical threshold value for DR was identified as 2.0 as in [21] and the obtained results are compared with this threshold. The whole DR values in the case of aging at U_0 are less than the threshold which means that the degradation is minor. However, in the case of aging at $2U_0$ and $3U_0$, the values of DR are higher than this threshold after 340 h of aging and become lesser for the remaining aging times.

Considering the assessment of degradation degree of XLPE under long-term electrical aging based on the proposed parameters (DI and DR), a detailed examination of the XLPE insulation was facilitated; hence, the parameters possess significant potential for assessing the state of the insulation.

Relative permittivity

The relative permittivity ε_r has been measured at the same time as the dielectric losses factor and in the same conditions. Figures 10(a to d) show the evolution of ε_r according to aging time and applied voltage.
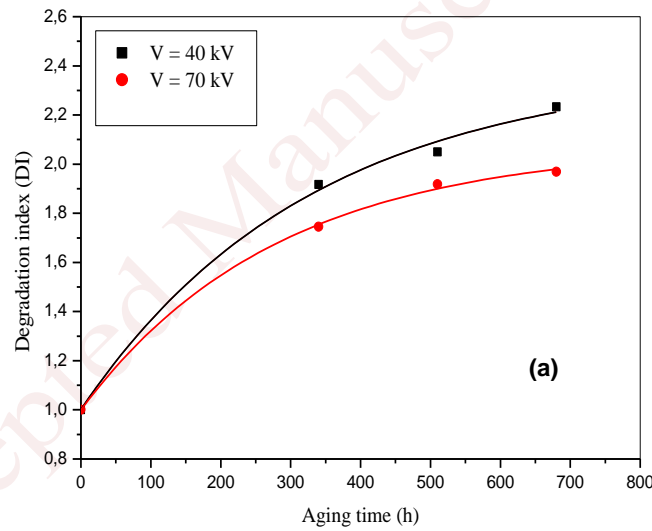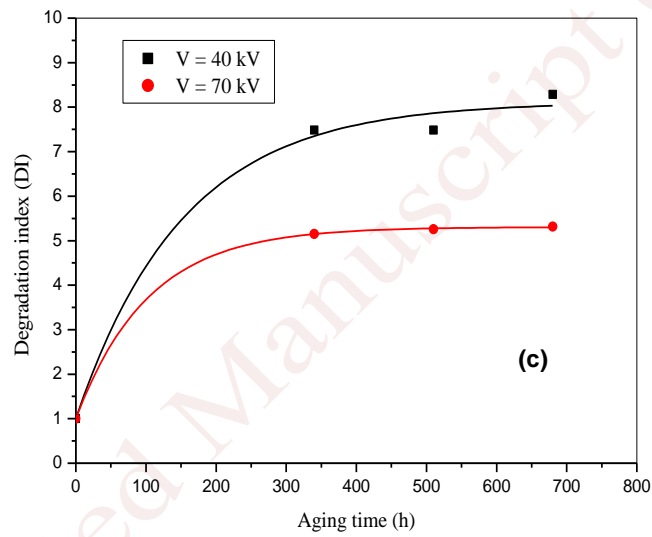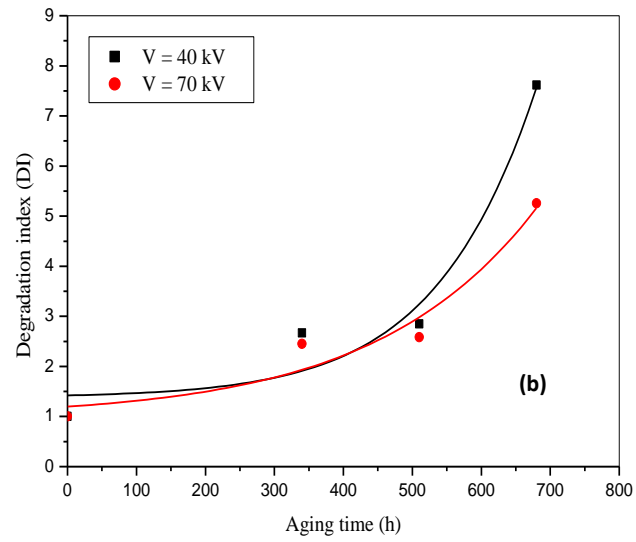
Figure 8. Degradation index vs aging time. (a) Aged at U_0, (b) Aged at $2U_0$ and (c) Aged at $3U_0$
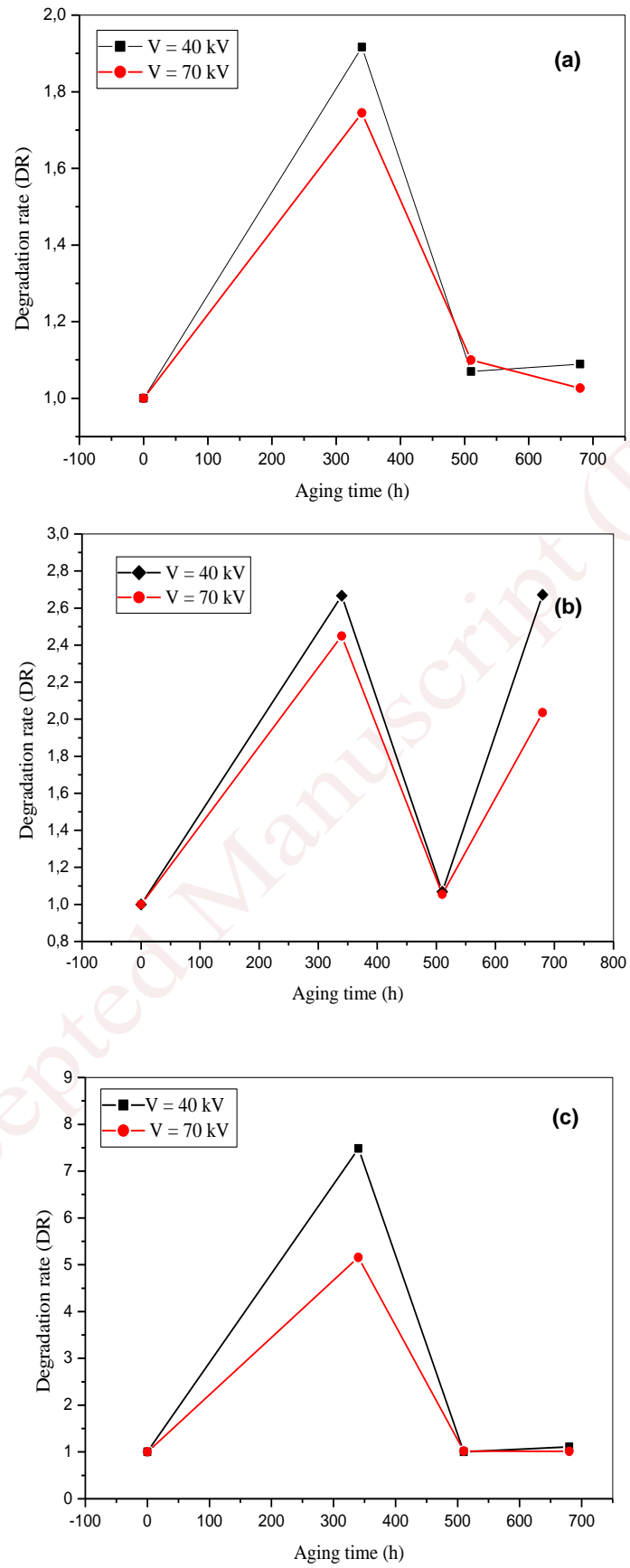
Figure 9. Degradation rate vs aging time. (a) Aged at U_0, (b) Aged at $2U_0$ and (c) Aged at $3U_0$.

The depicted curves have all a quite linear increase. Before aging, dielectric constant presents lower values than after aging for all applied voltages and it remains practically constant where its value still unchanged around 2.5. After 680 h of electrical aging, the permittivity values obtained around the specified voltage (30 kV-36 kV) are 2.93, 3.05 and 3.08, for samples aged at U_0, $2U_0$ and $3U_0$ respectively. It is established that when a low frequency electric field is applied, all the dipoles tend to line up with the field line, which induces a high value of permittivity [19]. In addition, we can interpret this increase by the shrinkage undergone by the material [22]. Indeed, the shrinkage of the XLPE leads to an increase in capacity and consequently an increase in relative permittivity.

Transverse resistivity

Resistivity is the main characteristic affected by the degradation of dielectric materials under long-term electrical aging. Figure 11 displays the changes in XLPE resistivity as a function of aging time for different values of aging voltage. As we can see, the XLPE resistivity decreases with respect to aging time

The resistivity decrease becomes worst when the aging voltage level is higher. The same behavior was observed for all three aging voltage levels. The observed behavior starts with a fast decrease after 174 hours of aging and leveled off after the rest of aging period. The resistivity decreases from 15.7_x10^{13} Ω.cm (before aging) to 9.064_x10^{13} Ω.cm, 8.577_x10^{13} Ω.cm and 6.489_x10^{13} Ω.cm after aging at U_0, $2U_0$ and $3U_0$ respectively.
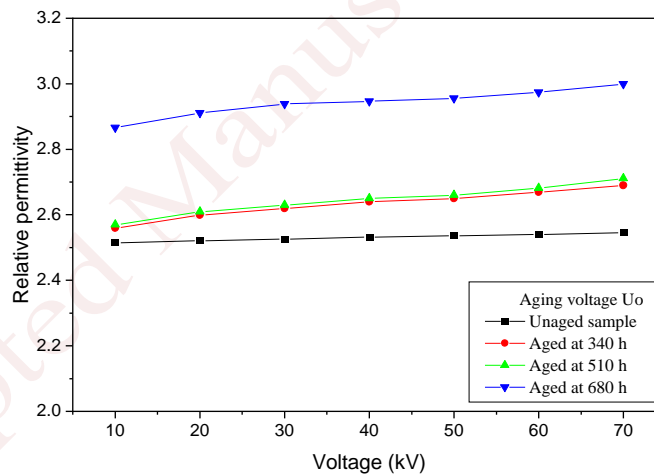

Figure 10a. Relative permittivity versus applied voltage before and after aging at U_o.
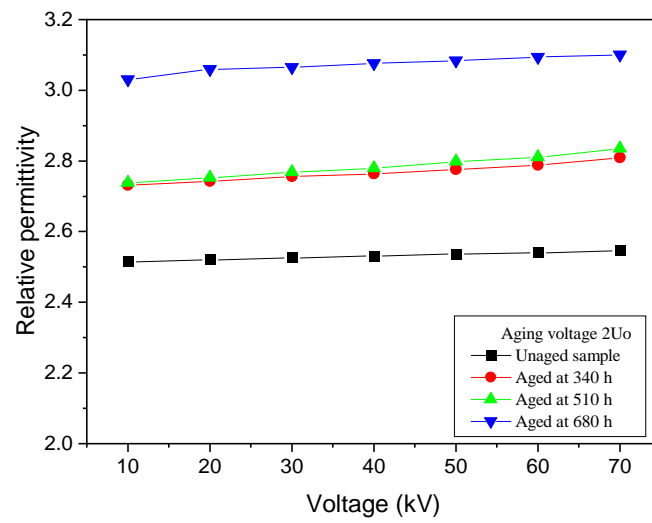
Figure 10b. Relative permittivity versus applied voltage before and after aging at $2U_o$.
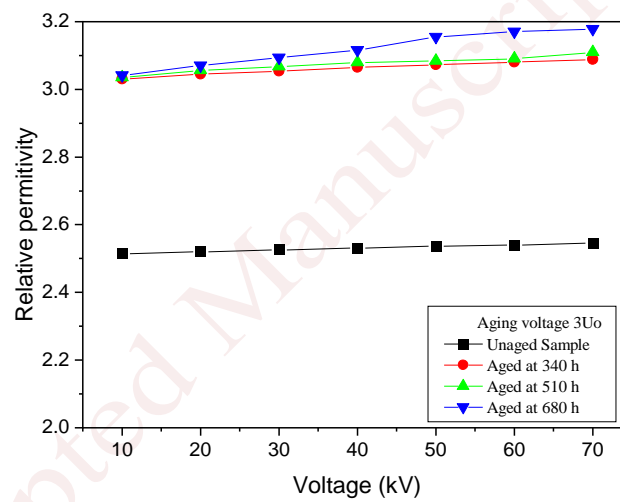

Figure 10c. Relative permittivity versus applied voltage before and after aging at $3U_o$.
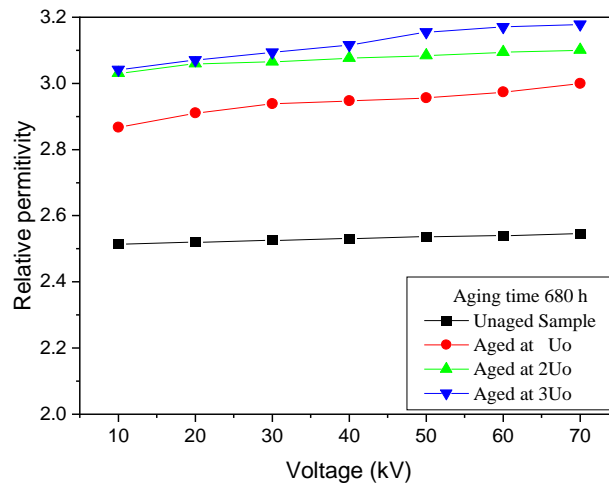
Figure 10d. Relative permittivity versus aging time and applied voltage.
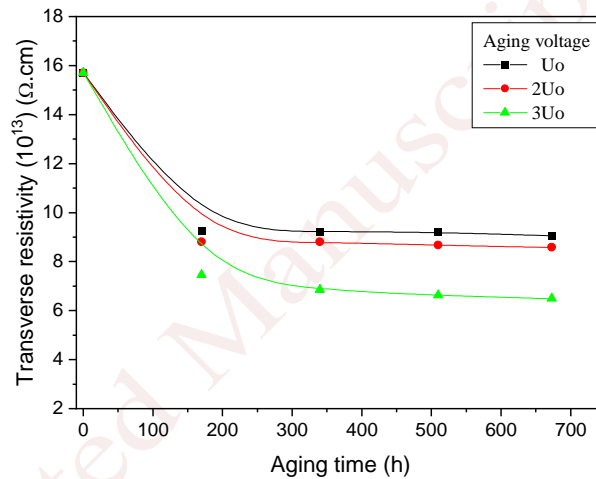

Figure 11. Transverse resistivity variations as a function of aging time for different aging voltages.

The diminution of resistivity with increasing aging time is due to the increasing of charge carrier's mobility [3]. Charge carriers are the result of many chemical reactions. One can admit that during long-term electrical aging, electrons gain more kinetic energy and become free hot electrons. These free hot electrons are accelerated by the permanent existing electric field which increases the collision probability with the molecular chains. This collision leads to the rupture of molecular chains and can lead to the formation of the unsaturated groups like C=C bonds [7]. The hot electrons become cold electrons and re-accelerated again by the applied electric field and form new hot electrons. The existing hot free electrons and the formed unsaturated groups lead to the diminution of the resistive character of the material and hence the decrease of its resistivity with increasing aging time.

Results of physico-chemical properties

To well understand the undergo degradation mechanisms under long-term electrical aging, several additional physico-chemical characterization techniques are used and the obtained results will be analyzed in this section.

Optical microscopy

The monitoring of the change in the surface state of XLPE using optical microscopy is illustrated in Figure 12. During aging under electrical stress, the surface of the insulator deteriorates with a cracked surface and cavities may appear.

Figure 12 illustrates the evolution of the surface state of the XLPE during electrical ageing. Optical microscopy performed with a (×50) magnification showed that long-term electrical aging leads to the appearance of defects on the surface of the material [22]. These defects represent holes and crack which due to the electromechanical effect of electrical stress. It was highlighted that electrical field has an electromechanical effect [23] involving the acceleration of chain breaks, particularly in the amorphous zone.
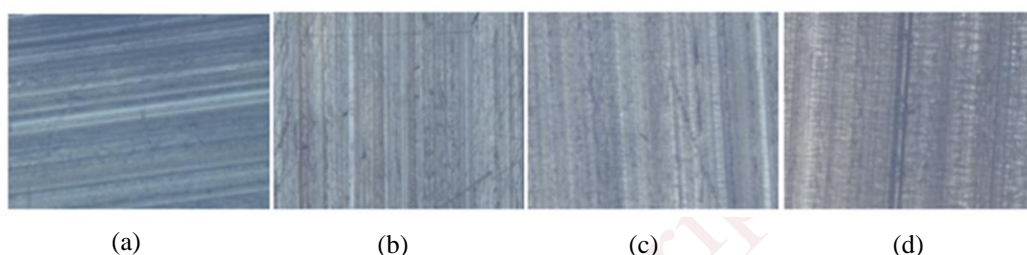

(a)	(b)	(c)	(d)

Figure 12. Optical microscopy images. (a) Before aging, (b) Aged at U_0 for 680 h, (c) Aged at $2U_0$ for 680 h, (d) Aged at $3U_0$ for 680 h.

ATR-FTIR Spectroscopy analysis

Figure 13 shows the FTIR spectrum of unaged and aged specimens in the wavenumber range of 4000–600 cm^{-1}. Unaged XLPE exhibits characteristic peaks of polyethylene structure at 719 cm^{-1} corresponds to the rocking methylene groups (–CH_2) [24,25].The peak at 1464 cm^{-1} is attributed to the wag vibration of (–CH_2). The other peaks at 2847 cm^{-1} and 2914 cm^{-1} correspond respectively to the symmetrical and asymmetric stretching vibration of the (–CH_2) groups [26,27]. The peaks at 1377 cm^{-1} are attributed to methyl group related to symmetric deformation vibration and symmetric valence vibration, respectively [27]. The absorption band around 1078 cm^{-1} is attributed to the presence of an antioxidant, such as Irganox [27], which could have been introduced into the polyethylene resin by the manufacturer. In addition, the presence of ester or aldehyde supported by the presence of the peak at 1737 cm^{-1} in the unaged sample indicates that oxidation process has taken place during manufacturing process. After aging, changes in the intensities of several peaks are noticed. This evolution may be due to the scissions of chains, which may be accompanied by cross-linking [24]. This behavior indicates also that the trans-conformation segments were decreased in population with aging, allowing depolymerization to occur. The diminution in the peaks intensities may be due to chain breaks induced by thermolysis of chain bonds or by oxidation. The other phenomenon after aging, the peak intensity increases, indicating the apparition of a competitive process to oxidation, namely, cross-linking. For each aging voltage level, we have remarked the formation of C=O carbonyl groups and an increase of the IR absorption band between 1500 cm^{-1} and 1800 cm^{-1}. The band at 2361 cm^{-1} is attributed to CO_2 species [28] increased with increasing voltage level. This increase is ascribed to gas phase and absorbed carbon dioxide produced as a consequence of oxidation reaction [29]. This behavior indicates also an increase in the photo-oxidation activity. Finally, the absorption zone of hydroxyl groups (–OH) is observed in the wavenumber

range of 3000–3500 cm^{-1}. Moreover, a slight increase in the absorption of (-OH) function of the hydroxyl groups could be observed after aging in the region between 3000 and 3500 cm^{-1} [30]. Furthermore, a significant increase in carbonyl groups was observed in the case of higher voltage level.

As seen in Figure 13, the FTIR spectra of samples exhibit some differences. The peaks between 2800 and 3000 cm^{-1} strongly decreased on the spectra of aged samples which clearly indicated that electrical aging affects the chain dynamics of XLPE samples. On the other hand, the absorption peak of carbonyl bands (C=O) at around 1700 cm^{-1} appeared at the spectrum of aged samples and increased with aging time and shifted to higher wavenumbers. This is due to the formation of oxidized species such as carbonyl groups, ketone, carboxylic acid and ester. This change in chemical structure and intensity of peaks could be related to surface erosion or roughness phenomena [29].

In addition to cross-linking, electrical aging of XLPE can induce the production of carbonyl groups. These components account for most of the oxidation products on the photo-oxidation of XLPE. From the FTIR spectra, it is possible to evaluate the oxidation level. Usually, two indexes can be assessed to obtain quantitative information on the oxidation level of XLPE. These two indexes are [24]: carbonyl index (*CI*) and double bond index (*DBI*). *CI* represents the relative intensity of the carbonyl band at 1737 cm^{-1} (aldehyde absorption) to the methylene band at 1464 cm^{-1} and can be calculated according to equation (5):

$$CI = \frac{Abs_{1737}}{Abs_{1464}} \tag{5}$$

Where Abs_{1737} and Abs_{1464} are the area under the peaks at 1737 cm^{-1} and 1464 cm^{-1}, respectively.

Whereas, *DBI* presents the relative intensity of the vinylidenes (C=C) unsaturated group at 1635 cm^{-1} to the methylene band at 1464 cm^{-1}. The *DBI* is calculated according to equation (6):

$$DBI = \frac{Abs_{1635}}{Abs_{1464}} \tag{6}$$

Where Abs_{1635} and Abs_{1464} are the area under the peaks at 1635 cm^{-1} and 1464 cm^{-1}, respectively.
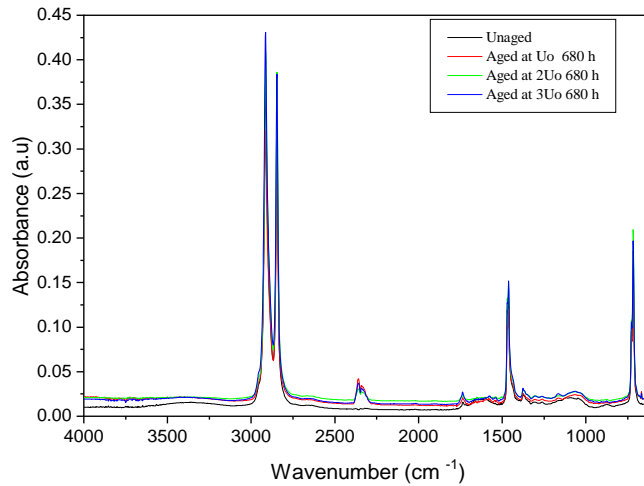
Figure 13. ATR-FTIR spectra of XLPE before and after long-term electrical aging.
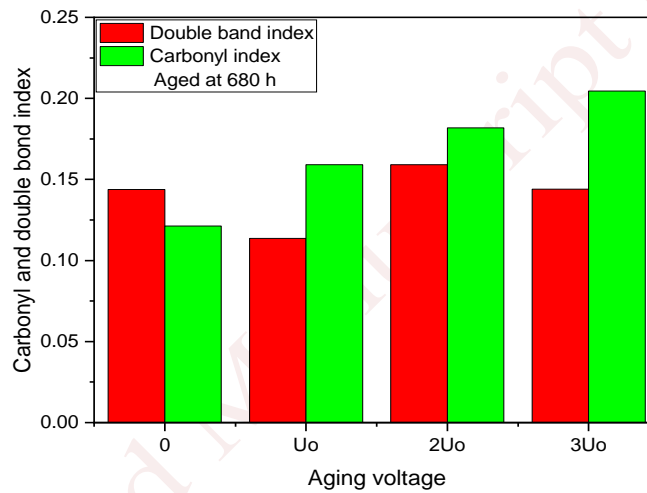

Figure 14. Carbonyl and double bond index for different aging voltage levels.

As shown in Figure 14 both aged and unaged samples contain carbonyl groups. The *DBI* and *CI* of virgin sample are, respectively, 0.1439 and 0.1212. After long-term aging of 680 h under different voltage levels, these indexes increase and reach the values of 0.1136 and 0.1590 for U_0, 0.1590 and 0.1818 for $2U_0$, and 0.1440 and 0.2045 for $3U_0$. A slight decrease in *DBI* is observed after aging at U_0 and maybe explained by the creation of new crosslink points at these double bands. It is well known that the energy of π band is very weak and can be broken easily to create new crosslink point under aging condition. This statement is in agreement with the hot set test results (see *Hot set test* section).

The increase of the concentration of carbonyl groups indicates an increase in the rate of oxidation reaction, and thus a growth in the generation of aging products [26]. Henceforth, the preferred mechanism associated with aging appears to be the one producing double bonds. This result is in agreement with the FTIR analysis related to the oxidation and depolymerization processes, which happened during the aging. Similar results were reported in previous studies [31,32].

XRD Results

Figure 15 shows the XRD patterns of aged and unaged samples. The semi-crystalline character of XLPE polymer is characterized by fundamental and secondary crystal peaks and a amorphous boss. The two fundamental peaks appear at $2\theta = 21.82°$ and $2\theta = 24.12°$ which are the characteristics of [110] and [200] plane lattice respectively, and the secondary crystal peak appears at $2\theta = 36.46°$ which matches to the lattice plane having [020] as Miller index [24,33].

It can be seen that the characteristic diffraction peaks of XLPE do not change their positions and yielded the same 2θ values after long-term electrical aging. This implies that no new crystalline phase is produced in the material. However, XRD results show that the shape and the intensities of the amorphous halo and crystal peaks present remarkable changes after long-term electrical aging which leads to the changes in the crystallinity degree of the material. The crystallinity degree can be calculated using the Hinrichsen's method [24]. By fitting the diffractogram into three Gaussian curves, the crystallinity degree χ (%) is given by the following relationship [24]:

$$x\left(\%\right) = \frac{Area2 + Area3}{Area1 + Area2 + Area3} * 100 \tag{7}$$

Where Area1 is area under the amorphous halo at $2\theta = 20.75°$, Area2 is area under the 1st principal crystal peak at about $2\theta = 21.82°$, and Area3 is area under the 2nd principal crystal peak at about $2\theta = 24.12°$.
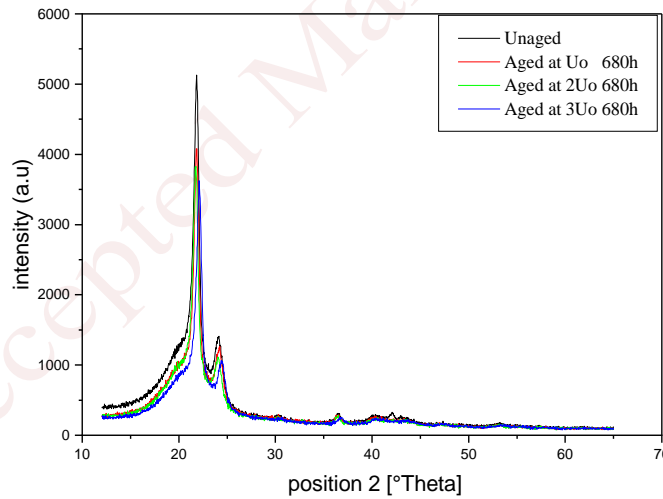
Figure 15. XRD spectra of XLPE samples aged at different voltage levels.

Figure 16 highlights that the tendency of crystallinity variation decreases with increasing voltage levels. It decreases from 22.06 % before aging to reach 21.14 %, 19.35 % and 18.28 % after 680 h of aging at U_0, $2U_0$ and $3U_0$ respectively. After long-term electrical aging the degradation becomes intense and the crystalline parts are themselves affected by the defects produced by oxidation (such as carbonyl and unsaturated groups) and chain scissions which prevent the tendency to recrystallization. Consequently, the amorphous regions are enlarged and consequently the crystallinity decreases dramatically [34]. In addition, one can admit that under electrical stress, collisions between hot electrons and folded molecular chains in the

crystallization regions can cause the breakage of molecular chains and the dissociation of spherulites, which is irreversible. This further exacerbates the decrease in crystallinity of XLPE, as well as the generation of holes on the spherulite.
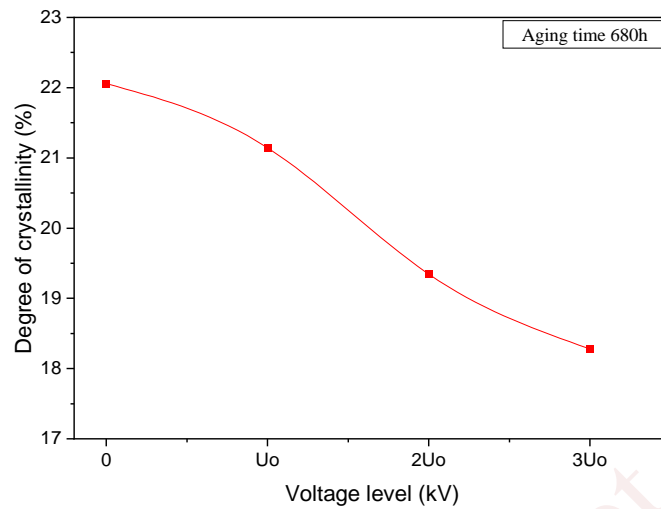

Figure 16. Crystallinity variation according voltage level after 680 h of aging.

Results of mechanical properties

Tensile experimental results

More analyses are given in this section and concerning the effect of long-term electrical aging on the mechanical properties of XLPE. We have measured tensile strength and elongation at break before and after 680 hours of electrical aging. The obtained results are listed in Table 2. The elongation at break and the tensile strength decrease as the aging voltage level increases. This decrease in mechanical properties is all the more accentuated as the level of aging stress is higher. The reduction in mechanical properties is directly linked to the oxidative degradation of the material, which is accompanied by chain breaks and whose speed increases with the rise in the voltage level. Chain breaks cause a decrease in the average molecular mass and in the cross-linking rate, thus causing embrittlement of the material. In the real case of aging, XLPE simultaneously undergoes chain scissions and cross-linking. Its mechanical properties then evolve according to the part played by each of these processes. But often the presence of oxygen (oxidation) leads to a predominance of skeletal cuts over cross-linking [24]. Moreover, the variations in mechanical properties are lower than the values prescribed by IEC 60811 [11] and thus meet the recommendations of the same standard.

Table 2. Mechanical properties of XLPE as a function of voltage level after 680 hours of aging.

	Elongation at rupture (L %)	Tensile strength (R N/mm^2)	ΔL (%)	ΔR (%)
Before aging	444.8	17.7	-	-
Aged at U_0	396.4	15.16	10.86	14.35
Aged at $2U_0$	383.5	14.70	13.78	16.95
Aged at $3U_0$	358.6	14.00	19.37	20.90

Hot set test

In order to study the effect of long-term electrical aging on the cross-linking degree of XLPE, hot set test measurements were carried out according to the given description in experimental section. The obtained results are listed in Table 3.

Table 3. Hot set test of XLPE as a function of voltage level after 680 hours of aging.

Voltage level	Before aging	Aged at U_0	Aged at $2U_0$	Aged at $3U_0$
Hot set test	64.50%	52.65%	58.50%	60.15%

The obtained results show a slight decrease in the hot set test elongation after aging for all aging voltage levels. This decrease reflects the enhancement of cross-linking degree of XLPE after long-term electrical aging. As the aging voltage level is less as the reduction in hot elongation is important and hence more enhancement in cross-linking degree. This may be explained by the existence of extensive hot electrons under high electric field and these hot electrons have enough energy to break macromolecules chains then reducing the cross-linking degree.

Multi-scale analysis and cross-correlation assessment

The important contribution of our study is the development of mathematical models relating XLPE characteristics at different scales. The presented multi-scale analysis presents a helpful tool to assess the existing cross-correlation between microscopic and macroscopic degradation markers. The used microscopic markers are carbonyl index and crystallinity, while the used macroscopic markers are the mechanical and dielectric properties. It is worth noting that the developed jointly curves concerns the samples aged for 680 h under different aging voltage levels (U_0, $2U_0$ and $3U_0$). The applied voltage is considered as a key parameter in our analysis. Since long-term electrical aging causes the exhaustion of the dielectric and mechanical properties, and the alteration of physico-chemical and microscopic structure of XLPE insulation, hence it is crucial to correlate different properties. In Figures 17a to 17e we have depicted the correlation curves between *tanδ*, partial discharges, transverse resistivity, elongation at rupture and tensile strength according to *CI*. The degree of correlation is evaluated by using the Pearson correlation coefficient (R-square). A high correlation coefficient between previous properties and *CI* was observed and combined evolution models can be generated. In Figures 17a and 17b pairs (*tanδ*, *CI*) and (partial discharges, *CI*) have a strong positive correlation with high values of Pearson coefficient as the aging voltage level increases. However pairs (resistivity, *CI*), (elongation at rupture, *CI*) and (tensile strength, *CI*) have a strong negative correlation. The values of R-square are summarized in Table 4. The strong positive correlation between dielectric properties and *CI* suggests the governance of same degradation process. This degradation process is based on the electro-thermal effect of high electrical field. The applied high voltage leads to an increase of insulation temperature leading to the oxidation phenomenon with the presence of oxygen. As the applied voltage is high, as the oxidation process is intense leading to the high values of *CI*. When *CI* increases the oxidized species are enough to alter the polarity of the material. The presence of polar oxidized species engenders more dielectric losses in the bulk of the material and excites more partial discharges. On the other hand, the presence of polar species enhance the conductive character of the polymer leading to the reduction of the transverse resistivity which explain well the strong negative correlation of this property with *CI* (Figure 17d).

The negative correlation between mechanical properties and *CI* (Figures 17d and 17e) put in evidence that, like in case of thermal aging process [33], oxidation has a direct impact on the mechanical behavior of XLPE in the case of electrical aging. It was highlighted [33] that oxidation leads to the chains scission and reduction of the molecular weight of the material. This process leads to the brittleness of the insulation and reduction of the mechanical properties. Furthermore, the generated combination models for pairs (*tanδ*, χ(%)), (partial discharges, χ(%)), (resistivity, χ(%)), (elongation at rupture, χ(%)) and (tensile strength, χ(%)) have been drawn in Figures 18a to 18e. Contrary to *CI*, a reverse behavior can be observed in all pairs with always strong correlation and high values of Pearson coefficient as the aging voltage level increases. The values of R-square for these pairs are summarized also in Table 4. *Tanδ* and partial discharges have a negative correlation with the measured crystallinity degree. These macroscopic dielectric properties increase with the decrease of crystallinity caused by long-term electrical aging. The higher the aging voltage level is; the important crystallinity decrease is. This correlation suggests that aging under high voltage stress creates more defects mainly in the amorphous part of the semi-crystalline XLPE polymer. These defects can be considered as the siege of more losses and initiate more partial discharges. Overall these negative correlations are in agreement with the electrical aging process. Besides, one can note a good positive correlation between the remaining pairs. The decrease in crystallinity degree, caused by long-term electrical aging leads to a decrease in mechanical properties of XLPE. It was highlighted [33] that mechanical properties are controlled by the crystalline structure of the semi-crystalline polymers. More the material becomes amorphous, more its resistance to the mechanical stress is less.

From all above figures, the generated joint evolution models for each case can be used in the prediction of a macroscopic parameter from the known microscopic parameter and vice-versa. The type and mathematical equation of each generated model is listed in Table 5.

Table 4. R-square values for different combination pairs.

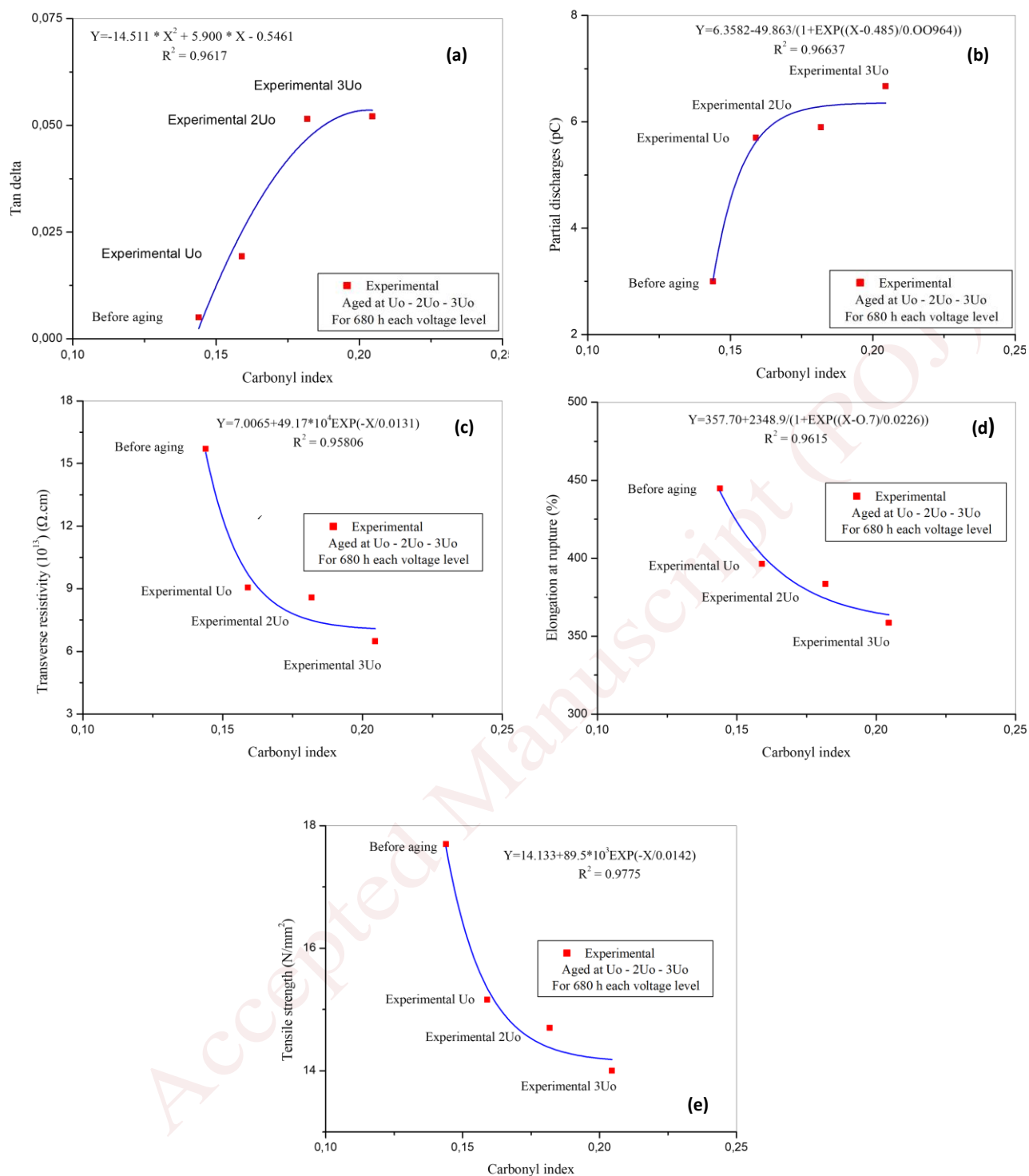|	R-square	
	CI	χ(%)
Tanδ	0.9617	0.9797
Partial discharges	0.9664	0.9621
Resistivity	0.9581	0.9566
Elongation at rupture	0.9615	0.9423
Tensile strength	0.9775	0.9727

Figure 17. Joint evolution models of dielectric and mechanical properties of XLPE vs *CI* (Aging level voltage is a tiers parameter).
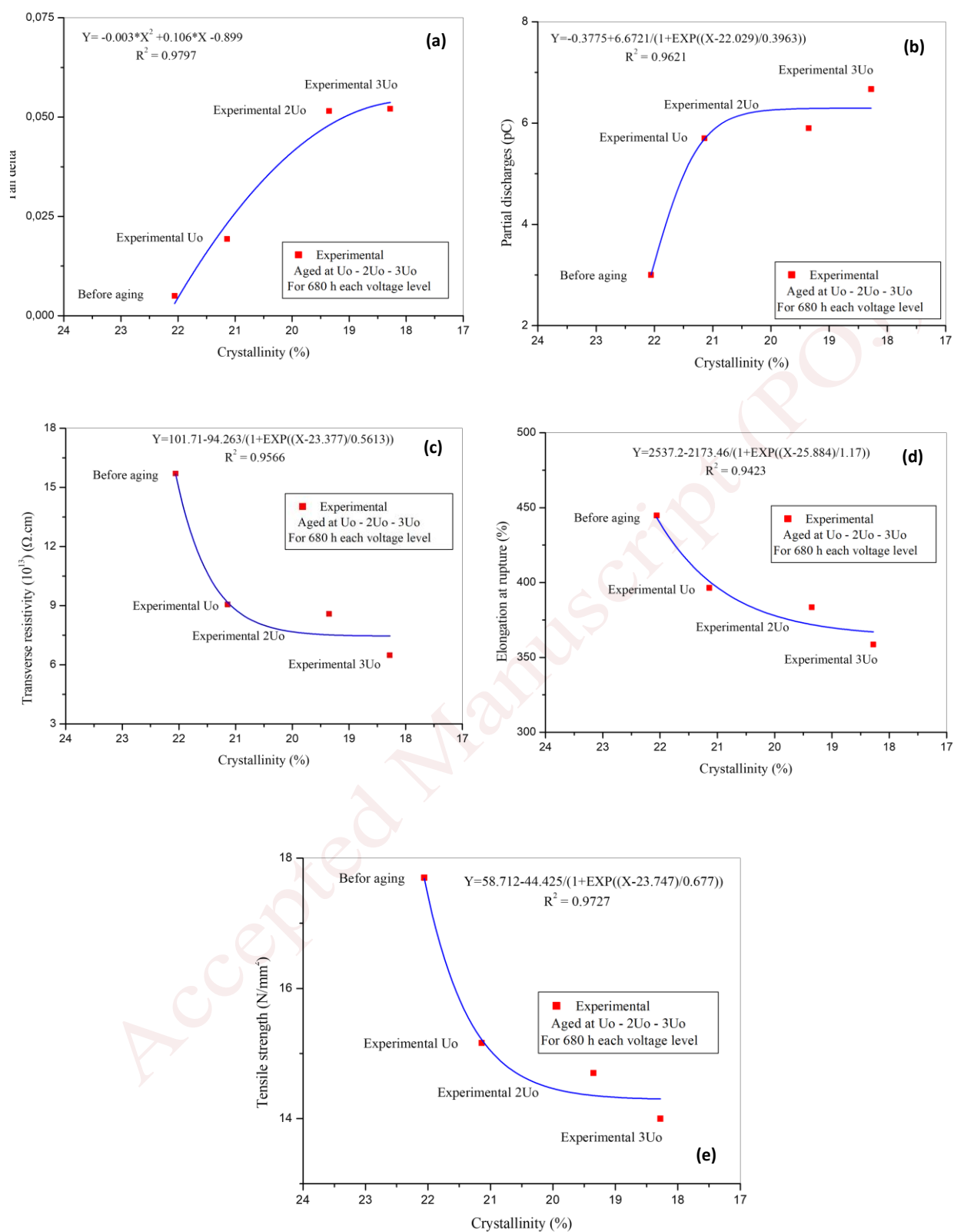
Figure 18. Joint evolution models of dielectric and mechanical properties of XLPE vs crystallinity (Aging level voltage is a tiers parameter).

Table 5. Generated mathematical models.

pairs	Type of model	Mathematical equation
(*Tanδ*, *CI*)	Polynomial	$y = -14.511x^2 + 5.9x - 0.5461$
(Partial discharges, *CI*)	Sigmoidal (Boltzmann)	$y = 6.3582 - \dfrac{49.863}{1 + e^{\left(\frac{x-0.485}{0.00964}\right)}}$
(Resistivity, *CI*)	Exponential	$y = 7.0065 + 49.17 \times 10^4 e^{\frac{-x}{0.01313}}$
(Elongation at rupture, *CI*)	Sigmoidal (Boltzmann)	$y = 357.7 + \dfrac{2348.9}{1 + e^{\left(\frac{x-25.884}{1.1697}\right)}}$
(Tensile strength, *CI*)	Exponential	$y = 14.133 + 89.5 \times 10^3 e^{\frac{-x}{0.0142}}$
(*Tanδ*, χ(%))	Polynomial	$y = -0.003x^2 + 0.106x - 0.899$
(Partial discharges, χ(%))	Sigmoidal (Boltzmann)	$y = -0.3775 + \dfrac{6.6721}{1 + e^{\left(\frac{x-22.0203}{0.3963}\right)}}$
(Resistivity, χ(%))	Sigmoidal (Boltzmann)	$y = 101.71 - \dfrac{94.2632}{1 + e^{\left(\frac{x-23.377}{0.5613}\right)}}$
(Elongation at rupture, χ(%))	Sigmoidal (Boltzmann)	$y = 2537.2 - \dfrac{2173.46}{1 + e^{\left(\frac{x-25.284}{1.1697}\right)}}$
(Tensile strength, χ(%))	Sigmoidal (Boltzmann)	$y = 58.712 - \dfrac{44.425}{1 + e^{\left(\frac{x-23.747}{0.6773}\right)}}$

CONCLUSION

The dielectric behavior of full-size HV XLPE insulation cables 36/66 kV under electrical stress was studied in this paper. The evolution of dissipation factor, relative permittivity, threshold voltage of partial discharges and transverse resistivity were used as diagnostic tools.

The obtained results show that the electrical stress considerably affects the dielectric properties of the material especially under severe stress conditions. Quantitatively, the following specific numerical results have been noticed:

- The increase in partial discharges occurring in the bulk of insulation material depends on the voltage level and the aging time. After 680 h of aging under U_0, $2U_0$ and $3U_0$, partial discharges increase from 2.9 pC to reach 5.7 pC, 5.9 pC and 6.67 pC respectively.
- The decrease in partial discharge threshold voltage and transverse resistivity are influenced by the AC voltage level values. Under the investigated voltage stresses, the obtained change rates on the PD voltage threshold, after 680 h of aging, were 18.5%, 24.6% and 41% respectively. Moreover, the resistivity decreases from 15.7×10^{13} (Ω.cm) (before aging) to 9.064×10^{13} (Ω.cm), 8.577×10^{13} (Ω.cm) and 6.489×10^{13} (Ω.cm) after aging at U_0, $2U_0$ and $3U_0$ respectively. This decrease depends closely on the aging time.
- The dissipation factor rises with increasing voltage level and aging time. Its value is higher after aging than before aging. After 680 h of aging it passes to 0.0193 after aging at U_0 and reaches 0.0515 and 0.0521 after aging at $2U_0$ and $3U_0$ respectively.
- The dielectric constant values are nearly constant with applied measurement voltage in all studied cases. However, it presents higher values after aging. The obtained values, after 680 h of aging, have a mean values around 2.9, 3.1 and 3.17 after aging at U_0, $2U_0$ and $3U_0$ respectively.

These various changes are mainly linked to the modification of the structure of the insulator due to the polarization phenomenon. This modification is more accentuated by the increase in voltage and the aging period

Therefore, these parameters can be used to evaluate and investigate the XLPE insulation cables quality under long-term electrical aging.

The above behavior was supported by the increase of carbonyl groups in the FTIR spectra of aged XLPE insulation (more than 68 % in the case of $3U_0$) indicating that oxidation process occurred during electrical aging process. In addition, it was found that long-term electrical aging could lead to reduction in the crystallinity degree of the material. However, XRD patterns indicated that no new crystalline phase is produced after long-term electrical aging.

REFERENCES

1. Boukezzi L, Rondot S, Jbara O, Ghoneim SSM, Boubakeur A, Abdelwahab SAM (2022) Effect of isothermal conditions on the charge trapping/detrapping parameters in e-beam irradiated thermally aged XLPE insulation in SEM. Materials 15: 1918 [CrossRef]
2. Seguchi T, Tamura K, Shimada A, Sugimoto M, Kudoh H (2012) Mechanism of antioxidant interaction on polymer oxidation by thermal and radiation ageing. Radiat Phys Chem 81: 1747-1751 [CrossRef]
3. Mecheri Y, Boukezzi L, Boubakeur A, Lallouani M (2000) Dielectric and mechanical behavior of cross-linked polyethylene under thermal aging. In: Annual Report Conference on Electrical Insulation and Dielectric Phenomena, Victoria, BC, Canada, 15-18 October 2000, pp.: 560-563 [CrossRef]
4. Jones J, Llewellyn J, Lewis T (2005) The contribution of field-induced morphological change to the electrical aging and breakdown of polyethylene. IEEE Trans Dielectr Electr Insul 12: 951-966 [CrossRef]
5. Stancu C, Notingher PV, Ciuprina F, NotingherJr. P, Castellon J, Agnel S, Toureille A (2009) Computation of the electric field in cable insulation in the presence of water trees and space charge. IEEE Trans Ind Appl 45: 30-43 [CrossRef]
6. Li W, Li J, Wang X, Li S, Chen G, Zhao J, Ouyang B (2014) Physicochemical origin of space charge dynamics for aged XLPE cable insulation. IEEE Trans Dielectr Electr Insul 21: 809-820 [CrossRef]
7. Li H, Xi Z, Xu L, Shan C, Nan M, Zhao L (2023) Research on the degradation in micro-structure and dielectric performance of XLPE cable insulation in service. J Mater Sci: Mater Electron 34: 1449 [CrossRef]
8. Wang Y, Ding Y, Yuan Z, Peng H, Wu J, Yin Y, Han T, Luo F (2021) Space-charge accumulation and its impact on high-voltage power module partial discharge under DC and PWM waves: Testing and modeling. IEEE Trans Power Electron 36: 11097-11108 [CrossRef]
9. IEC 60270 (2000) High voltage test techniques - Partial discharge measurements.
10. IEC 60840 (2020) Power cables with extruded insulation and their accessories for rated voltages above 30 kV (Um = 36 kV) and up to 150 kV (Um = 170 kV) –Methods and requirements test.

11. IEC 60811.501 (2012) Electrical and optical fiber cables – Test methods for non-metallic material – Part 501: Mechanical tests – Tests for determining the mechanical properties of insulating and sheathing compounds.

12. IEC 60811.507 (2012) Electrical and optical fiber cables – Test methods for non-metallic material – Part 507: Mechanical tests – Hot set test for cross-linked materials.

13. Medjdoub A, Boubakeur A (2005) Influence of electrical aging on the properties of cross-linked Polyethylene use as electrical insulation on underground power cables. IEEE Russia Power Tech conference, St. Petersburg, Russia, 27-30 June 2005 (PTC) [CrossRef]

14. Jonscher AK, Lacoste R (1984) On a cumulative model of dielectric breakdown in solids. IEEE Trans Electr Insul El-19: 567-577 [CrossRef]

15. Mason JH (1978) Disharges. IEEE Trans Electr Insul EI-13: 211-238 [CrossRef]

16. Han T, Li W, Zheng Z, Li Y, Chu J, Hao C (2025) Insulation aging evaluation method of high voltage cable based on dielectric loss characteristics. Energies 18: 1267 [CrossRef]

17. Larba M, Medjdoub A (2025) Electric field effect on the dielectric properties of insulating materials destined for medium voltage cable insulation. Electroteh Electron Autom 73: 62-69 [CrossRef]

18. Nelson JK (1983) Breakdown strength of solids. In: Engineering dielectrics volume IIA electrical properties of solid insulating materials: Molecular structure and electrical behavior, ASTM International, Bartnikas R, Eichhorn RM (eds), pp.: 445-520 [CrossRef]

19. Du BX, Li J (2014) Electrical and mechanical ageing behaviors of used heat-shrinkable insulation tubes. IEEE Trans Dielectr Electr Insul 21: 1875-1881 [CrossRef]

20. Crine J, Pelissou S, Parpal J (1991) Influence of insulation morphology, impurities and oxidation on some electric properties of cables. IEEE Trans Electr Insul 26: 140-145 [CrossRef]

21. Mustafa E, Ibrahim U, Ahmed N, Ahmed I, Abbasi AR, Nawaz A, Abbas MF, Tamus ZÁ (2026) Thermal degradation and multi-performance aging assessment of low voltage nuclear cable. Electr Power Syst Res 250: 112128 [CrossRef]

22. Hedir A (2017) Effects of electrical constraints and parameters environmental on dielectric properties insulation. PhD Thesis, Mouloud Mammeri University of Tizi-Ouzou, Algeria

23. Kahleras S, Boubakeur A, Boukezzi L (2018) Numerical study using FVM of three cavities within XLPE insulation of HV cables. 2018 International Conference on Electrical Sciences and Technologies in Maghreb (CISTEM), pp.: 1-5 [CrossRef]

24. Boukezzi L, Boubakeur A, Laurent C, Lallouani M (2008) Observations on structural changes under thermal ageing of crosslinked polyethylene used as power cables insulation. Iran Polym J 17(8): 611–624

25. Kuryndin I, Kostromin S, Mamalimov R, Chervov A, Grebennikov A, Bronnikov S (2022) Organic solvents effect on the physical and mechanical properties of polyethylene, Polyolefins J 9: 25-31

26. Dalal S, Gorur R, Dyer M (2005) Aging of distribution cables in service and its simulation in the laboratory. IEEE Trans Dielectr Electr Insul 12: 139-146 [CrossRef]

27. Melo Nobrega A, Barreira Martinez ML, Alencar de Queiroz AA (2013) Investigation and analysis of electrical aging of XLPE insulation for medium voltage covered conductors manufactured in Brazil. IEEE Trans Dielectr Electr Insul 20: 628-640 [CrossRef]

28. Aliahmad M, Nasiri Moghaddam N (2013) Synthesis of maghemite (γ-Fe2O3) nanoparticles by thermal-decomposition of magnetite (Fe3O4) nanoparticles. Mater Sci-Poland 31: 264-268 [CrossRef]

29. Ameen M, Raupp GB (1999) Reversible catalyst deactivation in the photocatalytic oxidation of diluteo-xylene in air. J Catal 184: 112-122 [CrossRef]

30. Hedir A, Slimani F, Moudoud M, Lamrous O, Durmus A, Fofana I (2022) Effects of electrical aging on the structural and physicochemical properties of crosslinked polyethylene (XLPE) cable insulation material. Eng Res Express 4: 015038 [CrossRef]

31. Ghunem RA, Tay L, Terrab H, El-Hag AH (2016) Analysis of service-aged 200 kV and 400 kV silicone rubber insulation in the Gulf region. IEEE Trans Dielectr Electr Insul 23: 3539-3546 [CrossRef]

32. Moghadam MK, Taheri M, Gharazi S, Keramati M, Bahrami M, Riahi N (2016) A study of composite insulator aging using the tracking wheel test. IEEE Trans Dielectr Electr Insul 23: 1805-1811 [CrossRef]

33. Smaida A, Mecheri Y, Boukezzi L, Bouazabia S (2025) Mechanical behavior of 60 kV HV XLPE insulation under thermal aging and cross-correlation assessment of degradation mechanisms. J Mech Sci Technol 39: 611-625 [CrossRef]

34. Qin S, Liu R, Wang Q, Chen X, Shen Z, Hou Z, Ju Z (2022) Study on the molecular structure evolution of long-term-operation XLPE cable insulation materials. Energy Rep 8: 1249-1256 [CrossRef]